Synthesis, crystal structure and spectroscopic characterization of a new cadmium phosphate, Na2Cd5(PO4)4

Teycir Ben Hamed, Amal Boukhris, Benoit Glorieux, Mongi Ben Amara

Synthesis, crystal structure and spectroscopic characterization of a new cadmium phosphate, $Na_2Cd_5(PO_4)_4$

Teycir Ben Hamed [a], Amal Boukhris [a], Benoit Glorieux [b], Mongi Ben Amara [a, *]

[a] UR Matériaux Inorganiques, Faculté des Sciences, Université de Monastir, Avenue de l'Environnement, 5019, Monastir, Tunisia
[b] Institut de Chimie de la Matière Condensée de Bordeaux, CNRS, Université de Bordeaux I, 87 Avenue du Dr. A. Schweitzer, 33608, Pessac-Cedex, France

ARTICLE INFO

Article history:
Received 30 November 2018
Received in revised form
17 July 2019
Accepted 20 August 2019
Available online 23 August 2019

Keywords:
Phosphate
Crystal structure
Vibrational spectroscopy
Cadmium photoluminescence

ABSTRACT

A novel cadmium phosphate compound $Na_2Cd_5(PO_4)_4$ was synthesized in single crystal and in powder forms using flux and Pechini methods, respectively. It was then characterized by single crystal X ray diffraction, vibrational spectroscopy and photoluminescence measurements. This compound crystallizes in the monoclinic system with space group $P2_1/a$, lattice parameters $a = 8.276(1)$ Å, $b = 9.301(3)$ Å, $c = 9.455(2)$ Å, $\beta = 111.82\ (1)^\circ$ and $Z = 2$. The structure consists of $(Na_{3/4},Cd_{1/4})O_7$, $(Cd_{3/4},Na_{1/4})O_6$ and CdO_x ($x = 6, 7$), polyhedra and PO_4 tetrahedra linked through common corners or edges giving rise to a novel type of complex three dimensional framework. This structure could be described in terms of $[(Na_{3/4},Cd_{1/4})_2(Cd_{3/4},Na_{1/4})_2Cd_3O_{16}]_\infty$ layers stacked parallel to the (2 0 3) plane and interconnected both directly and via PO_4 tetrahedra by sharing common corners and edges. Vibrational spectroscopy and cadmium photoluminescence were analyzed according to the structural results.

1. Introduction

Complex phosphates containing divalent cations are of increasing interest due to their large crystallographic characteris tics and their potential applications as host materials for optically active ions. By adjusting the composition and the structure of a compound, its optical features can be easily modulated as it has been observed in numerous family of phosphate compounds such as apatite (Ca, Sr, Ba)$_{10}(PO_4)_6Cl_2$:(Eu, Mn) [1–3] and glaserite Na_2(Ca, Sr, Ba)$Mg(PO_4)_2$:(Eu) [4–6]. Inorganic cadmium phosphate Na_2CdPO_4F doped by trivalent europium was also recently inves tigated for its optical properties [7].

In the search of new phosphate compounds as host materials for optically active rare earth ions, a close examination of the literature data dedicated to phosphate of sodium and divalent cations (M^{2+}) shows that among the large number of reported structures, three of them adopt the general formula $Na_2M_5(PO_4)_4$. Their structural disparities are mainly due to the different coordination numbers adopted by the M^{2+} cations. $Na_2Ca_5(PO_4)_4$ [8,9] was obtained from hydroxyapatite after high temperature treatments. This compound crystalizes in the hexagonal system with space group $P6_1$, a 10.6336 Å, c 21.6422 Å and Z 6. The a and c axes are, respectively, the double and triple of those of the subcell typical of α phases in the A_2XO_4 and $ABXO_4$ systems. Authors suggest, for the calcium and sodium atoms, similar environments to those observed in $Ca_7(PO_4)_2(SiO_4)_2$. $Na_2Mg_5(PO_4)_4$ [10] was prepared at 673K in a sealed silver tube under internal pressure of 100 MPa. It crystalizes in the triclinic system with space group $P\bar{1}$, a 7.923 Å, b 8.124 Å, c 5.160 Å, α 90.41°, β 101.92°, γ 110.71° and Z 1. The $Na_2Mg_5(PO_4)_4$ structure is constructed from two types of MgO_6 octahedra and one distorted MgO_5 polyhedron, connected through two kinds of PO_4 tetrahedra. The concomitance of two different coordination numbers (5 and 6) for magnesium has been reported for other phosphate compounds such as $Mg_3(PO_4)_2$ [11]. $Na_2Zn_5(PO_4)_4$ [12] was obtained as crystals by melt method. This compound crystallizes in the orthorhombic system with space group Pbcn, a 10.381 Å, b 8.507 Å, c 16.568 Å and Z 4. The structure exhibits an anionic three dimensional framework built up from ZnO_4 and PO_4 tetrahedra. The lowest plausible value (4) for the coordination number of Zn was also observed in several phosphate compounds such as $NaZnPO_4$ [13].

To our knowledge, no similar compound has been reported in the literature for other divalent elements. Thus, as a contribution to the study of the above system, we report here on the synthesis of the sodium cadmium phosphate $Na_2Cd_5(PO_4)_4$. This novel com pound was furthermore characterized by X ray diffraction,

* Corresponding author.
E-mail address: mongi.benamara@fsm.rnu.tn (M. Ben Amara).

vibrational and photoluminescence spectroscopies. The knowledge of the crystal structure of this phase is necessary for a subsequent study of its luminescent properties.

2. Experimental

2.1. Synthesis

Single crystals of $Na_2Cd_5(PO_4)_4$ were grown in a flux of sodium dimolybdate $Na_2Mo_2O_7$ with an atomic ratio P:Mo 2:1. Appropriate amounts of Na_2CO_3, $Cd(NO_3)_2{\cdot}4H_2O$, $(NH_4)H_2PO_4$ and $H_{24}N_6Mo_7O_{24}$ were dissolved in concentrated nitric acid and the derived solution was heated to dryness at 373 K. The resulting dry residue was ground in an agate mortar, transferred into a platinum crucible and heated at 873 K for 24 h until the decomposition products (NH_3, CO_2) were removed. After being finely ground, the mixture was melted for 1 h at 1173 K before being slowly cooled at a rate of $10°.h^{-1}$ down to 673 K, and then brought back to room temperature. The mixture, obtained by washing the final product with warm water in order to dissolve the flux, consists of essentially colorless and quasi prismatic single crystals.

A polycrystalline sample of the title compound was successfully synthesized by the Pechini method [14]. The preparation was undertaken in the following steps (1): 0.213 g of $NaCO_3$, 3.116 g of $Cd(NO_3)_2{\cdot}4H_2O$ and 1.067 g of $(NH_4)_2HPO_4$ were dissolved in diluted nitric acid. (2): 0.22 g of critic acid and 0.1 g of ethylene glycol were added to the obtained solution. (3): the limpid solution was kept at 373K for 8 h under continuous stirring. (4): The transparent gel was heated at 423K leading to a brown resin. (5): A white powder was obtained by calcining the precursor for 12 h successively at 673K and 873K, then for 24 h at 1173K.

2.2. X ray diffraction

The purity of the synthesized powder was examined through its X ray diagram collected in the range $5° \leq 2\theta \leq 120°$ on a PANatycal diffractometer using Cu(Kα) radiation (λ 1.5406 Å) (Fig. 1).

The structure was determined by X ray diffraction performed on a crystal of dimensions $0.07 \times 0.14 \times 0.22$ mm^3. Data collection was recorded by a CAD4 Enraf Nonius X ray diffractometer using a graphite monochromated MoKα radiation (λ 0.71073 Å). The unit cell parameters and the orientation matrix were determined on the basis of 25 intense reflections in the range $9.41° \leq \theta \leq 14.03°$. A total of 1462 unique reflections were collected with a maximum 2θ of 54° (R_{int} 0.059) using the ω 2θ scan mode. Only 1163 reflections were considered observed according to the criterion [$I > 2\sigma(I)$]. The intensity data were corrected for the Lorentz and polarization effects and then for absorption by the empirical method using DIFABS program ($T_{min,max}$ 0.28, 0.56) [15]. On the basis of systematic absences and statistic of intensity distribution, the space group was determined to be $P2_1/a$.

The structure was solved by direct method using SIR 92 program [16] which revealed the positions of the cadmium atoms. The remaining atomic positions were located by Fourier synthesis alternating with least squares refinement based on F^2 (SHELXL 97) [17]. A possible disordered distribution of Cd^{2+} and Na^+ in M(1) and M(2) sites was considered due to their similar ionic radii ($r(Cd^{2+})$ 0.95 Å and $r(Na^+)$ 1.02 Å [18]. The refinements based on this hypothesis converged to a distribution in M(1) and M(2) sites close to the atomic ratios of Cd:Na 1:3 and 3:1, respectively. The occupancy factors of Cd and Na atoms in the considered sites were then fixed to (0.25Cd + 0.75Na) and (0.75Cd + 0.25Na), respectively. A last refinement, including all atomic coordinates and anisotropic thermal parameters, converged at R_1 0.036 and wR_2 0.086 for the observed reflections, which confirms consequently the proposed formula. Crystal data, experimental conditions for intensity measurement, and refinement parameters are given in Table 1. Final atomic coordinates and equivalent isotropic temperature factors are reported in Table 2 and selected bond distances in Table 3. All calculations were performed using the Wingx software package [19].

Further details of the crystal structure investigation may be obtained from the Fachinformationszentrum Karlsruhe, D 76344 Eggenstein Leopoldshafen (Germany), on quoting the depository

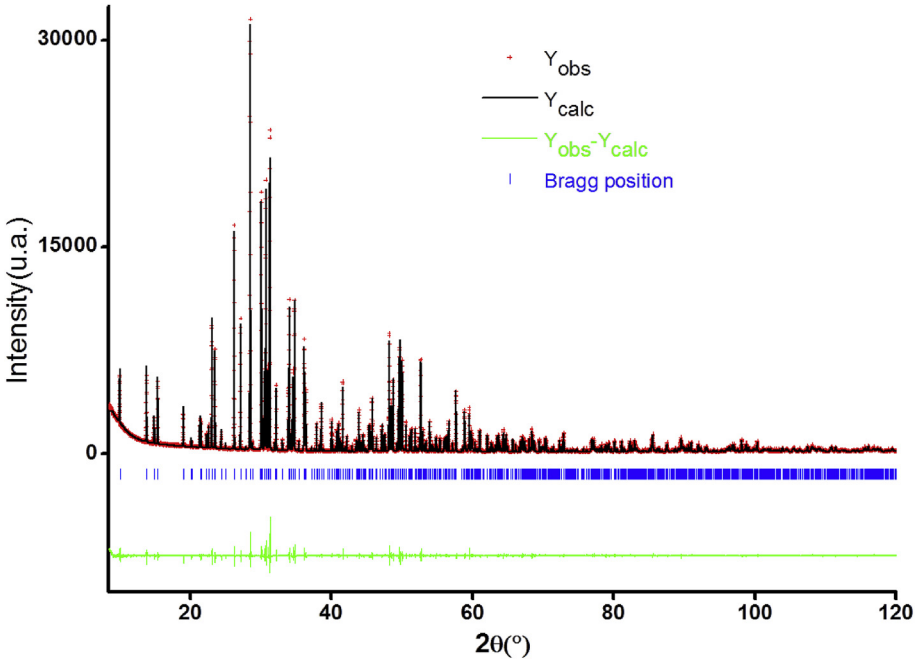

Fig. 1. X-ray powder diffraction pattern of $Na_2Cd_5(PO_4)_4$.

Table 1
Details of the data collection and structural refinement for $Na_2Cd_5(PO_4)_4$.

Crystal data	
Chemical formula	$Na_2Cd_5(PO_4)_4$
Formula weight (g/mol)	987.86
Crystal system	Monoclinic
Space group	$P2_1/a$
a (Å)	8.276(1)
b (Å)	9.301(3)
c (Å)	9.455(2)
β (°)	111.82(1)
V (Å^3)	675.66
Z	2
ρ_{cal} (Kg/m^3)	4.86×10^3
Intensity measurements	
Crystal dimensions (mm)	$0.07 \times 0.14 \times 0.22$
Temperature (K)	293(2)
Apparatus	CAD4 (Enraf-Nonius)
λ MoKα (Å)	0.71073
Monochromator	Graphite
μ (mm ^{1})	8.375
Scan mode	$\omega/2\theta$
θ range	$2{,}32 \leq \theta \leq 26{,}97$
Unique reflections; R_{int}	1462; 0.059
Observed reflections ($I > 2\sigma(I)$)	1163
Indices	$-1 \leq h \leq 10$; $-1 \leq k \leq 11$; $-12 \leq l \leq 12$
$F(000)$	900
Structure solution and refinement	
Intensity correction	Lorentz-Polarization
Absorption correction	Refdelf
$T_{min;\ max}$	0.28; 0.56
Resolution method	Direct method
Agreement factors ($I > 2\sigma(I)$)	R_1 0.036; wR_2 0.086; S 1.06
Number of refined parameters	124
Extinction coefficient	0.0037(7)
Weighting scheme	W $1/[\sigma^2(F_o^2) + (0.0470P)^2 + 0.419P]$ where P $(F_o^2 + 2F_c^2)/3$
$(\Delta\rho)_{max;min}$ (e. Å ^{3})	1.536; −1.397

number CSD 433733.

In order to confirm the proposed cationic distribution, the final structural model was examined with bond valence sum (BVS) cal culations using Chardi (CD) method [20]. The charge distribution was calculated using the CHARDI IT program [21]. The corre sponding results are reported in Table 4. This method was used to validate structures, as in the case where some atoms are disordered in the same crystallographic site [22]. In the present structure, the calculated valences of all the sites are consistent with their formal charges. In particular, the valence of 1.239 and 1.729 calculated for the M(1) and M(2) sites, respectively, are in a good agreement with 1.25 and 1.75 predicted by the structural refinement.

Table 2
Atomic coordinates and equivalent thermal parameters U_{eq} (Å^2) for $Na_2Cd_5(PO_4)_4$.

Site	Atom	$x(\sigma)$	$y(\sigma)$	$z(\sigma)$	$U_{eq}(\sigma)$[a]
M(1)	¾Na+¼Cd	0.3258(2)	0.1339(2)	0.8926(2)	0.0144(3)
M(2)	¼Na+¾Cd	0.5365(1)	0.9958(1)	0.6881(1)	0.0103(2)
Cd(1)	Cd	0.4517(1)	0.6460(1)	0.5983(1)	0.0128(2)
Cd(2)	Cd	0	0	0	0.0107(2)
P(1)	P	0.3085(2)	0.3328(2)	0.6370(2)	0.0069(4)
O(11)	O	0.3738(7)	0.8645(6)	0.4858(6)	0.0114(11)
O(12)	O	0.4499(7)	0.4077(7)	0.5961(7)	0.0129(11)
O(13)	O	0.8024(7)	0.1076(6)	0.7890(6)	0.0105(11)
O(14)	O	0.3308(7)	0.1690(6)	0.6468(6)	0.0119(12)
P(2)	P	0.2994(2)	0.8030(2)	0.8545(2)	0.0071(4)
O(21)	O	0.2380(7)	0.7114(7)	0.7071(6)	0.0135(12)
O(22)	O	0.6463(8)	0.6010(7)	0.8527(7)	0.0186(13)
O(23)	O	0.4527(7)	0.9011(7)	0.8624(6)	0.0154(12)
O(24)	O	0.3594(7)	0.7045(7)	0.9949(6)	0.0131(12)

[a] *Ueq* is defined as one third of the trace of the orthogonalized *Uij* tensor.

2.3. Vibrational spectroscopy

The Raman scattering experiments were carried out on a multichannel X−Y Dilor spectrometer using the 514.5 nm line of a Spectra Physics argon ion laser. The Raman spectrum was recorded at room temperature in the wavenumber range 60−4000 cm^{-1} with resolution of about 2 cm^{-1}. Infrared spectrum was obtained at room temperature by the KBr pellet method in the spectral range of 400−4000 cm^{-1} using a BioRad 575C FT IR spectrometer. The spectral resolution was about 3 cm^{-1}.

2.4. Photoluminescence

Photoluminescence properties were analyzed using a spectro fluorimeter SPEX FL212. Excitation spectra were corrected for the variation of the incident flux as well as emission spectra for the transmission of the monochromator and the response of the pho tomultiplier. This equipment is composed of a 450 W xenon lamp, an excitation double monochromator, a sample holder, an emission double monochromator and a photomultiplier tube.

3. Results and discussion

3.1. Description of the structure

Atomic representation of asymmetric unit and projection of the structure on the (100) plane are given in Fig. 2a and b, respectively. The structure of $Na_2Cd_5(PO_4)_4$ can be described as a three dimensional network of CdO_x and MO_x polyhedra (M Na or Cd and x 6 or 7) linked together through the PO_4 tetrahedra. From the projection of the structure along the b axis (Fig. 3), one can

Table 3
Selected interatomic distances (Å) and angles (°) for $Na_2Cd_5(PO_4)_4$.

PO_4 tetrahedra			
P(1) O(11)	1.552(5)	P(2) O(21)	1.549(6)
P(1) O(12)	1.530(6)	P(2) O(22)	1.544(6)
P(1) O(13)	1.558(5)	P(2) O(23)	1.542(6)
P(1) O(14)	1.533(6)	P(2) O(24)	1.536(6)
<P(1)-O>	*1.543*	*<P(2)-O>*	*1.543*
DI(PO)	*0.0101*		*0.0049*
O(12)-P(1)-O(14)	112.4(3)	O(23)-P(2)-O(21)	111.0(3)
O(12)-P(1)-O(13)	111.1(3)	O(24)-P(2)-O(22)	110.8(3)
O(12)-P(1)-O(11)	110.3(3)	O(24)-P(2)-O(21)	110.0(3)
O(14)-P(1)-O(13)	110.0(3)	O(24)-P(2)-O(23)	108.4(3)
O(14)-P(1)-O(11)	107.2(3)	O(23)-P(2)-O(22)	108.4(4)
O(11)-P(1)-O(13)	105.5(3)	O(22)-P(2)-O(21)	108.3(3)
<O-P(1)-O>	*109.42*	*<O-P(2)-O>*	*109.48*
DI(OPO)	*0.0185*		*0.0110*
$M(1)O_7$ polyhedron		$M(2)O_6$ polyhedron	
M(1)-O(24)	2.263(6)	M(2)-O(23)	2.196(6)
M(1)-O(14)	2.363(6)	M(2)-O(11)	2.247(5)
M(1)-O(23)	2.382(6)	M(2)-O(14)	2.270(5)
M(1)-O(23)	2.469(7)	M(2)-O(13)	2.297(6)
M(1)-O(13)	2.577(6)	M(2)-O(11)	2.418(5)
M(1)-O(22)	2.589(7)	M(2)-O(21)	2.511(6)
M(1)-O(24)	2.850(6)		
<M(1)-O>	*2.499*	*<M(2)-O>*	*2.323*
DI(MO)	*0.0606*		*0.0401*
$Cd(1)O_7$ polyhedron		$Cd(2)O_6$ polyhedron	
Cd(1) O(12)	2.216(6)	Cd(2) O(24) × 2	2.221(6)
Cd(1) O(11)	2.273(6)	Cd(2) O(13) × 2	2.287(5)
Cd(1) O(12)	2.325(6)	Cd(2)-O(22 × 2	2.355(6)
Cd(1) O(22)	2.382(6)		
Cd(1) O(21)	2.430(6)		
Cd(1) O(21)	2.573(6)		
Cd(1) O(14)	2.618(6)		
<Cd(1)-O>	*2.402*	*<Cd(2)-O>*	*2.288*
DI(MO)	*0.0547*		*0.0204*

distortion indices: *DI(PO)* $(\sum_{i\ 1}^{4}|PO_i - PO_m|)/4PO_m$

DI(OPO) $(\sum_{i\ 1}^{6}|OPO_i - OPO_m|)/6OPO_m$

formally isolate cationic polyhedra layers stacked parallel to the plane (2 0−3). Two successive layers equivalent by the a glide plane perpendicular to the b axis are interconnected via the PO_4 tetra hedra. One layer is depicted separately in Fig. 4, it consists of an alternating assemblage of two kinds of chains both propagating along the b axis. The $[M(2)Cd(1)O_{11}]_\infty$ chains are formed by alter nating $Cd(1)O_7$ and $M(2)O_6$ polyhedra sharing common corners and edges. The $[M(1)_2Cd(2)O_{16}]_\infty$ chains are consisted by $M(1)_2O_{12}$ units of edge sharing $M(1)O_7$ polyhedra, which are connected to

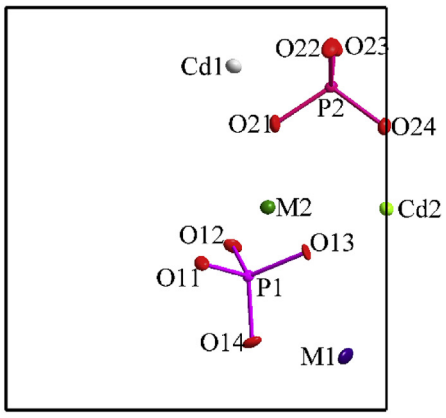

(a)

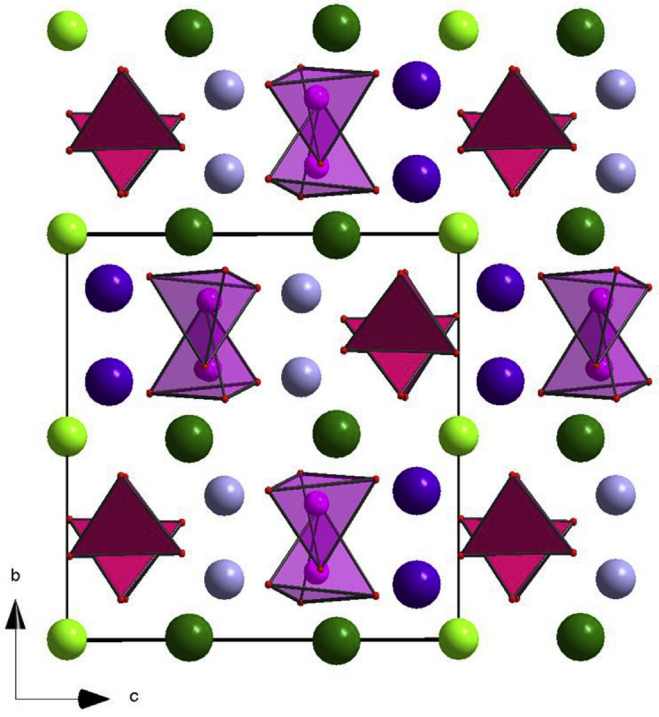

(b)

Fig. 2. (a) Atomic representation of asymmetric unit (b) Projection of the $Na_2Cd_5(PO_4)_4$ structure along the [100] direction (M(1): violet; M(2): olive; Cd(1): mauve; Cd(2): Green; $P(1)O_4$: purple; $P(2)O_4$ pink).

Table 4
Charge distribution (CD) sum calculation of $Na_2Cd_5(PO_4)_4$.

Cation	*q*	Q	Anion	*q*	Q
M(1)	1.250	1.239	O(11)	−2.000	−2.145
M(2)	1.750	1.729	O(12)	−2.000	−2.098
Cd(1)	2.000	2.000	O(13)	−2.000	−1.930
Cd(2)	2.000	2.025	O(14)	−2.000	−2.021
P(1)	5.000	4.886	O(21)	−2.000	−1.778
P(2)	5.000	5.134	O(22)	−2.000	−1.930
			O(23)	−2.000	−2.050
			O(24)	−2.000	−2.049
σ 0.080 σ 0.117					

Q: computed charge; *q*: formal oxidation number;

Charge dispersion: σ $\sum_{i\ 1}^{n}[(q_i - Q_i)^2/N - 1]^{1/2}$

$Cd(2)O_6$ octahedra through common edges. Thereby, although the framework is highly complex, it can be easily described by considering that all the CdO_x and MO_x polyhedra are linked directly by sharing either corners or edges to form $M(1)_2M(2)_2Cd_3O_{16}$ units connected to each other either directly or through PO_4 tetrahedra and leading to the formation of a compact structure.

Considering cadmium−oxygen distances below 3.0 Å as sug gested by Donnay and Allmann [23], the Cd(1) and Cd(2) sites are surrounded by seven and six oxygen atoms (Fig. 5) with Cd−O distances ranging from 2.216(6) Å to 2.618(6) Å and from 2.221(6) Å to 2.355(6) Å, respectively. These distances are closer to those found in the interstitial voids of the $NaCd_4(PO_4)_3$ (2.186−2.462 and 2.230 to 2.421 Å) [24] than to the Cd−O distances in the polyhedral

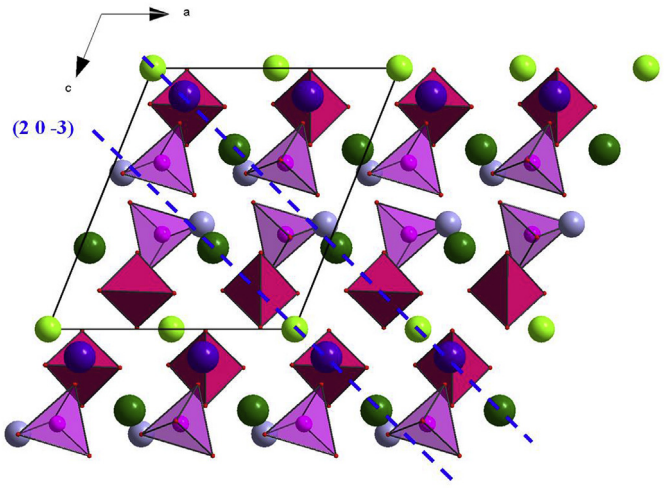

Fig. 3. Projection of the $Na_2Cd_5(PO_4)_4$ structure along the [010] direction (M(1): violet; M(2): olive; Cd(1): mauve; Cd(2): Green; $P(1)O_4$: purple; $P(2)O_4$ pink).

cluster $[Cd_2(VO_4)_3]^{5-}$ observed in $KCd_4(VO_4)_3$ (2.150–2.362 and 2.154 to 2.303 Å) [25].

Because M(2) site is statistically occupied by (3/4Cd + 1/4Na), the average bond length <M(2) O> 2.323 Å is much closer to 2.310 Å than to 2.40 Å observed for the six coordinated Cd and Na atoms in $NaCdPO_4$, respectively [26]. The M(1) site is also statisti cally occupied by Cd and Na, with atomic ratio Cd:Na 1:3. Furthermore, this site has a [6 + 1] coordination, with six short distances between 2.263 Å and 2.589 Å and a long distance of 2.850 Å. As a consequence, the mean distance <M(1) O> 2.499 Å is larger than observed within M(2) site.

The $P(1)O_4$ and $P(2)O_4$ tetrahedra present P–O distances included between 1.530(6) and 1.558(5) Å. Their mean distances <P(1)–O> <P(2)–O> 1.543 Å are consistent with that pre dicted by Baur and in a good accordance with those usually observed in monophosphate groups [27–29]. The minimum, maximum and average tetrahedral O–P–O angles are respectively: O–P(1) O 105.5, 112.4 and 109.42°; O–P(2) O 108.3, 111.0 and 109.48°. This dispersion reflects that the $P(1)O_4$ tetrahedron is more distorted than the $P(2)O_4$ one. The difference in the cationic distribution around the two tetrahedra (Fig. 6) seems to be corre lated with the disparity between their distortions. The calculated distortion indices corroborate this result as shown in Table 3.

The main feature of this structure is the existence of different kinds of sites for cadmium and sodium atoms. The Cd(1) and Cd(2) sites are full occupied by cadmium atoms whereas the M(1) and M(2) sites are statistically occupied by sodium and cadmium atoms. The cadmium atoms have slightly distorted octahedral environ ments in Cd(2) and M(2) sites, while their environments consist of seven oxygen atoms in the Cd(1) and M(1) sites. This cationic dis tribution is very different from those reported for phosphates with similar composition. Indeed, $Na_2Mg_5(PO_4)_4$ adopts the triclinic system with space group $P\bar{1}$. Its structure consists of a three dimensional framework built up from two kinds of MgO_6 octa hedra and one distorted MgO_5 polyhedron sharing edges and cor ners and linked to each other through the PO_4 tetrahedra [10]. $Na_2Ca_5(PO_4)_4$ is a member of the nagelschmidtite compounds family which crystallizes in the hexagonal system with space group $P6_1$. Its structure involves NaO_9, CaO_x and $(Na,Ca)O_x$ (x 6–8) polyhedra linked together through the monophosphate groups [9]. $Na_2Zn_5(PO_4)_4$ crystallizes in the orthorhombic system with space group Pbcn. Its structure is made up of five types of tetrahedra, three ZnO_4 and two PO_4, linked to each other by only shared cor ners to form a three dimensional anionic framework [12].

3.2. Vibrational analysis

The $Na_2Cd_5(PO_4)_4$ structure belongs to the spectroscopic group C_{2h}. The primitive cell is centrosymmetric containing two formula units. Two cadmium atoms as well as all phosphorus, oxygen and sodium ones are located on the general 4e position (C_1 symmetry); whereas the remainder of cadmium atoms occupies the 2a position

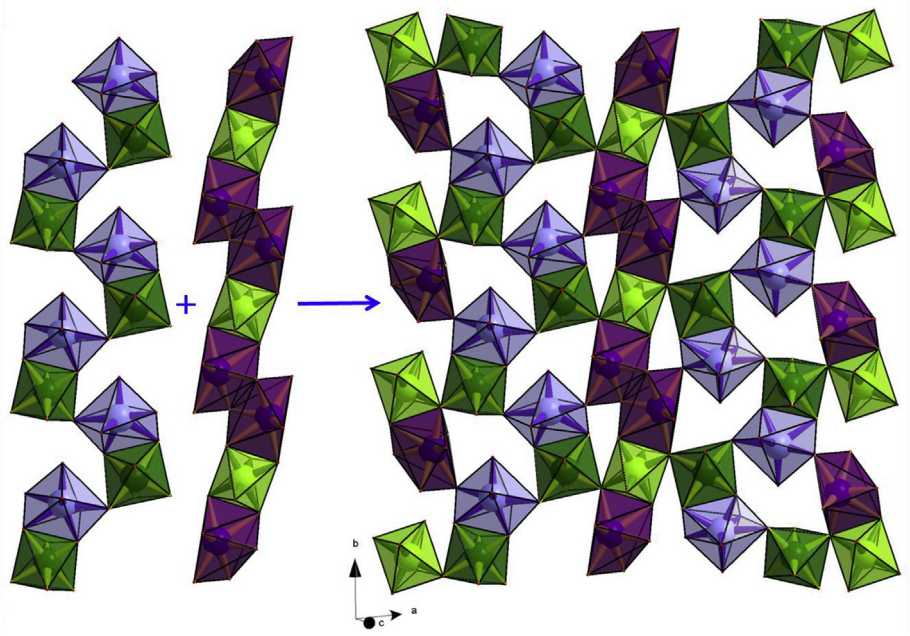

Fig. 4. $[M(1)_2M(2)_2Cd_3O_{16}]_\infty$ layer formed by an alternating assemblage of $[M(2)Cd(1)O_{11}]_\infty$ and $[M(1)_2Cd(2)O_{16}]_\infty$ chains ($M(1)O_7$: violet; $M(2)O_6$: olive; $Cd(1)O_7$: mauve; $Cd(2)O_6$: Green).

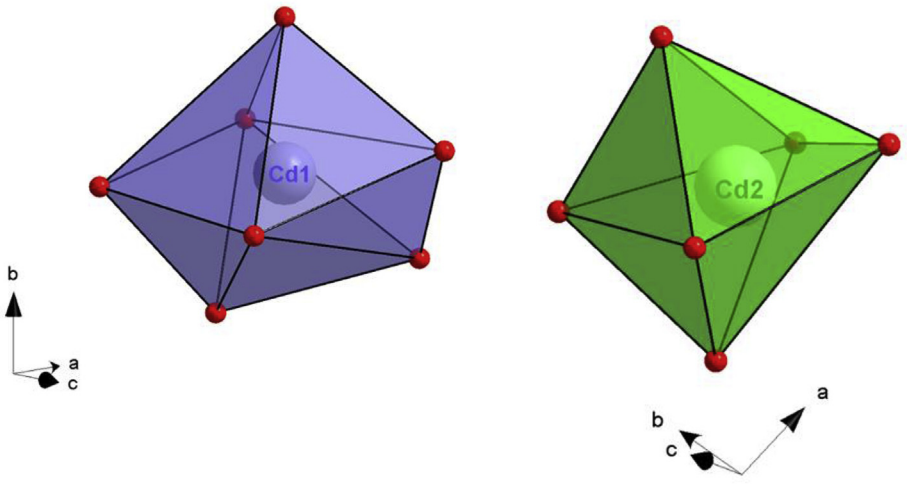

Fig. 5. Oxygen environments of the cadmium atoms in the $Na_2Cd_5(PO_4)_4$ structure (Cd(1)O_7: mauve; Cd(2)O_6: Green).

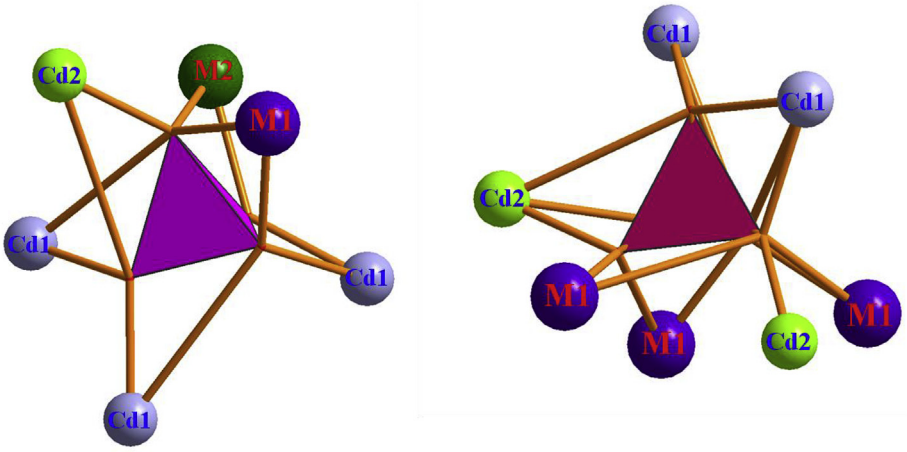

Fig. 6. Cationic environments of the P(1)O_4 (left) and P(2)O_4 (right) tetrahedra in $Na_2Cd_5(PO_4)_4$ for maximum distance d(P-M) 3.30 Å.

(C_i symmetry). The $Na_2Cd_5(PO_4)_4$ cell contains therefore 54 atoms that give 54×3 162 vibrational modes in which are included three acoustic modes. From the factor group analysis with the standard correlation method [30] a total number of 159 optical modes are predicted with the irreducible representation:

$$\Gamma_{opt} \quad 41A_u + 40B_u + 39A_g + 39B_g$$

Separating vibrational modes into internal (PO_4^{3-}) and external (lattice) modes is supported by previous works [31,32]. Internal vibrations consist of intramolecular stretching and bending mo tions of the PO_4^{3-} anions. Vibrational analysis for an undistorted PO_4^{3-} anion with T_d symmetry leads to 4 modes, which are one A_1 [ν_1; $\nu_s(PO_4)$], one E [ν_2; $\delta_s(PO4)$] and two T_2 [$\nu_{3,4}$; $\nu_{as}(PO_4)$ and $\delta_{as}(PO_4)$] modes with frequencies appearing at 938, 420, 1017 and 567 cm^{-1}, respectively [33]. All of them are Raman active, whereas only ν_3 and ν_4 are infrared active. In the $Na_2Cd_5(PO_4)_4$ lattice, the two non equivalent tetrahedral PO_4^{3-} groups are located on general C_1 positions. Their vibrational behavior can be analyzed by means of the site group method [34]. Due to the symmetry diminution from T_d to C_1, all vibrational modes become infrared and Raman active and degeneracies are totally removed, as can be seen from Table 5.

Thus, for each tetrahedral PO_4^{3-} group, we expect, for the stretching vibrations, eight Raman active modes: $2\nu_1(A_g + B_g) + 6\nu_3(3A_g+3B_g)$ and eight IR active modes: $2\nu_1(A_u + B_u) + 6\nu_3(3A_u+3B_u)$. As for the bending vibrations, we expect ten Raman active modes: $4\nu_2(2A_g+2B_g) + 6\nu_4(3A_g+3B_g)$ and ten IR active modes: $4\nu_2(2A_u+2B_u) + 6\nu_4(3A_u+3B_u)$. The external modes consist of the translational vibrations of Na^+, Cd^{2+} and PO_4^{3-} ions and of rotational vibrations of the PO_4^{3-} groups. The corre sponding irreducible representations are obtained by subtraction as follows:

$$\Gamma_{ext.} \quad \Gamma_{opt.} \quad \Gamma_{\text{int.}} \quad 23A_u + 22B_u + 21A_g + 21B_g$$

The IR and Raman spectra of the synthesized powder sample (Fig. 7) are typical of a monophosphate [35,36]. The Raman spec trum of $Na_2Cd_5(PO_4)_4$ is dominated by a strong band situated

Table 5
Correlation between the point group T_d, the site-group C_l and the factor group C_{2h}.

Vibrational mode	T_d	C_1	C_{2h}
symmetric stretching $\nu_1 \approx 938$ cm ^{1}	A_1	A	$A_g + B_g + A_u + B_u$
symmetric bending $\nu_2 \approx 420$ cm ^{1}	E	2A	$2A_g + 2B_g + 2A_u + 2B_u$
antisymmetric stretching $\nu_3 \approx 1017$ cm ^{1}	T_2	3A	$3A_g + 3B_g + 3A_u + 3B_u$
antisymmetric bending $\nu_4 \approx 567$ cm ^{1}	T_2	3A	$3A_g + 3B_g + 3A_u + 3B_u$

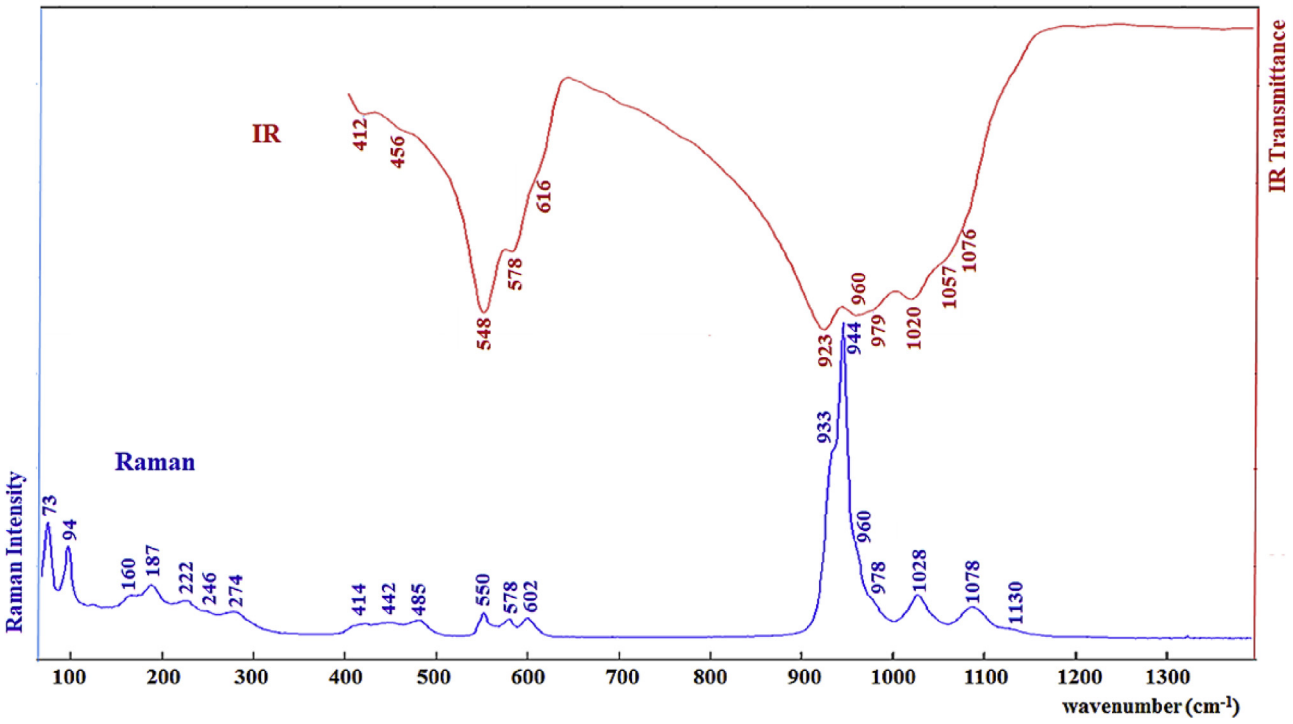

Fig. 7. Vibrational (IR and Raman) spectra of $Na_2Cd_5(PO_4)_4$.

around 940 cm^{-1}. The deconvolution process applied on this band leads to four intense bands centered at 931, 939, 946 and 957 cm^{-1} and one weak shoulder at 979 cm^{-1} (Fig. 8). The four intense bands appearing in the non degenerate stretching mode (ν_1) region can be assigned to the $2(A_g + B_g)$ modes in agreement with the factor group analysis. The shoulder at 979 cm^{-1} in addition to the bands at 1000, 1028, 1049, 1088 and 1129 cm^{-1} are attributed to the asym metric stretching mode (ν_3). Similar observations are reported for phosphate compounds such as $Na_2MMg(PO_4)_2$ with M Ba, Sr, Ca [37]. The weak bands, observed in the wavenumber ranges 380 500 cm^{-1} and 530 630 cm^{-1}, are characteristic of the bending modes (ν_2) and (ν_4), respectively. Due to the complex overlapping of the ν_2, ν_3 and ν_4 bands, distinction of A_g and B_g symmetries is not possible. Consequently, the decomposition of the Raman spectrum in the 400–1200 cm^{-1} spectral range allowed only 20 Raman active modes to be observed out of a total of 36 expected from the factor group analysis. In sum, the decomposition of the intense non degenerate band ν_1 into four components, in addition to the large splitting of the weak $\nu_{2\text{-}4}$ bands, confirms the presence of two distinct PO_4^{3-} groups as determined from X ray studies. Bands observed below 300 cm^{-1} are ascribed to lattice modes. Decom position of the Raman spectrum in the 60–400 cm^{-1} spectral range

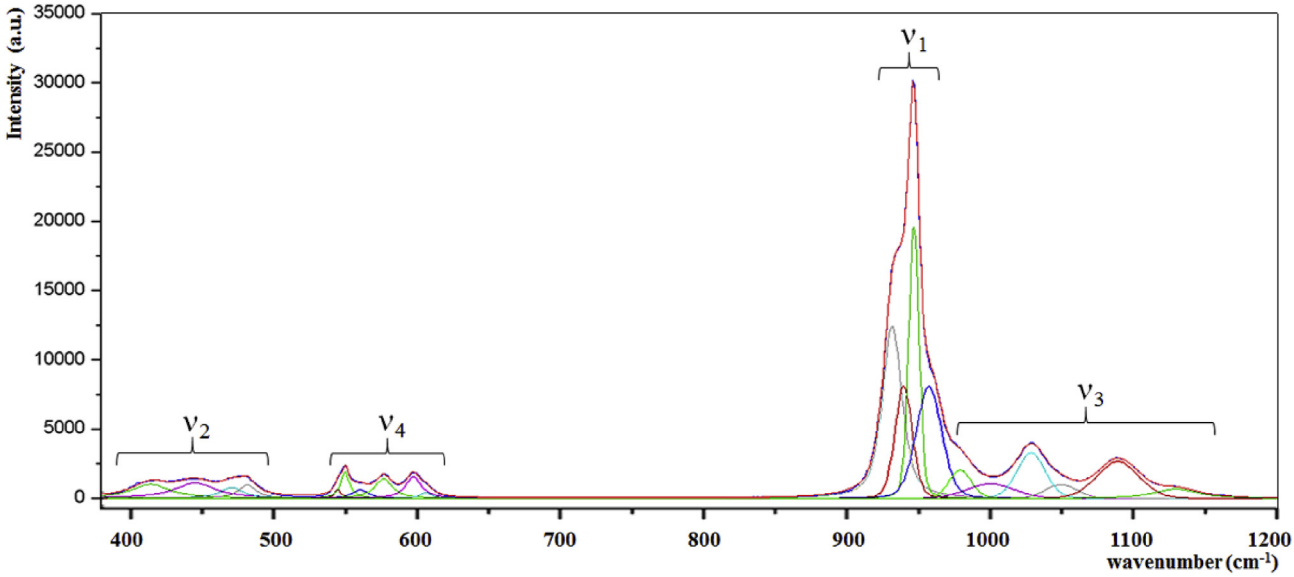

Fig. 8. Decomposition of the Raman spectrum of $Na_2Cd_5(PO_4)_4$ in the 400 1200 cm^{-1} spectral range.

allowed only 13 Raman active modes to be observed (graph not shown). Moreover, it is difficult to assign them without polarization measurements (non available). Former studies of phosphates showed that the rotational and translational modes of the PO_4^{3-} groups were located in a broad wavenumber range, 120–300 cm^{-1} and active modes associated with Na^+ ions are observed around 50 cm^{-1} [38]. Thereby, among bands observed for lattice modes of $Na_2Cd_5(PO_4)_4$, those appearing in the wavenumber range 122–275 cm^{-1} can be attributed to PO_4^{3-} groups rotational and translational modes while bands, which are observed between 61 and 111 cm^{-1}, can be associated to translational modes of the Na^+ and Cd^{2+} ions. Table 6 summarizes the main data from the deconvolution of Raman spectrum of $Na_2Cd_5(PO_4)_4$.

Because of the broad overlapping of the bands, the infrared spectrum cannot be precisely assigned. However, some results that are consistent with the interpretation of the Raman spectrum can be reported (Table 6). The observed bands and shoulders in the wavenumber range 1076–979 cm^{-1} are attributed to asymmetric triply degenerate mode (ν_3). The bands at 960 and 923 cm^{-1} are assigned to symmetric P–O stretching mode (ν_1). Note that the occurrence of the two distinct symmetric stretching bands with large splitting corroborates the presence of two distinct PO_4 tetrahedra. The asymmetric triply degenerate mode (ν_4) and sym metric doubly degenerate mode (ν_2) of O–P–O bandings are observed in the wavenumber ranges 616–548 cm^{-1} and 456–412 cm^{-1}, respectively.

3.3. Cd^{2+} photoluminescence

Photoluminescence spectra of the compound $Na_2Cd_5(PO_4)_4$ are shown in Fig. 9. The emission is performed by setting the excitation wavelength at 210 nm. The excitation is performed by setting the emission wavelength at 610 nm.

The emission spectrum can be described as a broad band from 550 nm to 700 nm. It is due to a Cd^{2+} center. While Cd^{2+} lumi nescence is not well known, it can be assimilated to the lumines cence of Ag^+ cation. The luminescence, in the visible range, is due to the $4\,d^{10}\ 4\,d^9\ 5s$ transition [39].

The observed broad band cannot be fit by a single Gaussian

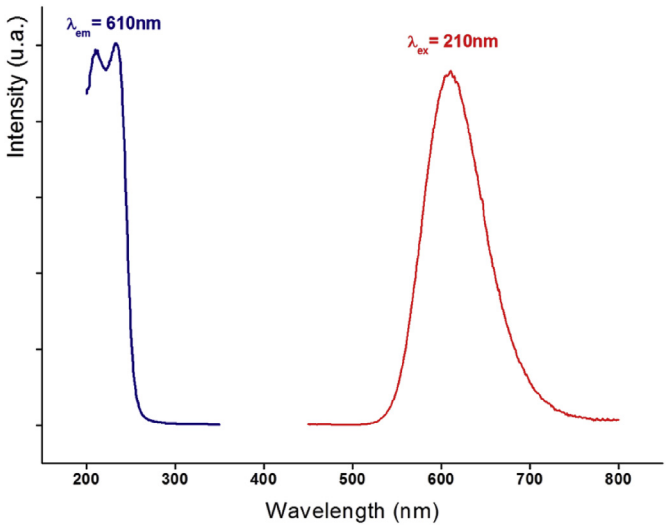

Fig. 9. Photoluminescence excitation (blue line) and emission (red line) spectra of $Na_2Cd_5(PO_4)_4$.

shape (in an energy abscise format). At least, two Gaussian bands are necessary to fit the band; see Fig. 10. The resulting bands are relevant of two ranges of crystal field surrounding cadmium cat ions. The band at the highest intensity (0.0017 eV) is related to cadmium site having the lowest crystal field. The band at the lowest intensity (0.00155 eV) is related to cadmium site having the highest crystal field. Regarding the crystallographic description (Figs. 2 and 3) and the interatomic distance (Table 3), the band at 0.0017 eV is relevant of the six coordinated cadmium sites Cd(2) and M(2). And the band centered at 0.00155 eV is relevant of the seven coordinated cadmium sites Cd(1) and M(1).

The difference of the broadness between these two bands could be related to the difference of average Cd–O interatomic distances between each site. Cadmium in the M(2) site and in the Cd(2) site get an interatomic distances Cd–O of, respectively, 2.323 Å and 2.288 Å. Cadmium in the M(1) site and in the Cd(1) site get an

Table 6
Spectral data (cm^{-1}) and vibrational band assignments for $Na_2Cd_5(PO_4)_4$.

Internal modes			External modes	
assignment	Raman	IR	assignment	Raman
ν_3; $\nu_{as}(PO_4)$	1129		$T(PO_4^{3-}) + R(PO_4^{3-})$	275
	1088	1076		248
	1049	1057		225
	1028	1020		204
	1000			187
	979	979		165
				136
ν_1; $\nu_s(PO_4)$	957	960		122
	946			
	939		$T(Cd^{2+}) + T(Na^+)$	111
	931	923		95
				91
ν_4; $\delta_{as}(PO_4)$	608	616		73
	599			61
	578	578		
	562			
	552			
	547	548		
ν_2; δ_s(PO4)	484			
	473			
	447	456		
	416	412		

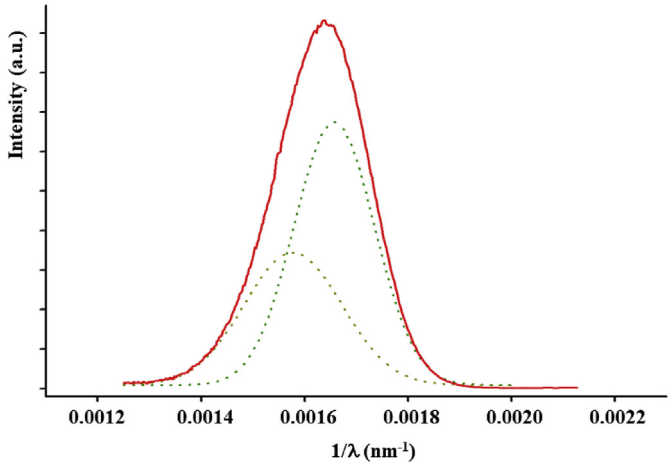

Fig. 10. Emission spectra of $Na_2Cd_5(PO_4)_4$ under λ_{exc} 220 nm deconvoluted in two Gaussian components.

interatomic distance of, respectively, 2.499 Å and 2.402 Å. The difference of interatomic distances Cd—O between M(2) and Cd(2) is only 1.5%, while it is 4% of difference for cadmium in M(1) and Cd(1) sites. So, the band at 0.0017 eV can be considered as composed of two Gaussian bands related to the six coordinated cadmium Cd(2) and M(2) sites. Since the crystal fields surrounding these cadmium cations are similar, the two bands are almost superposed. The band at 0.00155 eV, relevant of the seven coordinated cadmium Cd(1) and M(1) sites, can also be considered as composed of two Gaussian bands. Since the crystal fields surrounding these cadmium cations are quite different, the bands are more separated, inducing a broadening of the overall band.

Furthermore, the absence of additional bands confirms the purity of the powder sample. Indeed, in case of Cd cluster, of cadmium in interstitial position, additional photoluminescent phenomena would appear [40]. Photoluminescence is quite more sensible than X ray diffraction. So, the single phase state of the powder sample is clearly identified.

4. Conclusion

The sodium cadmium phosphate $Na_2Cd_5(PO_4)_4$ was synthesized and its crystal structure investigated. It is a new member within the $Na_2M_5(PO_4)_4$ series of compounds. Its unique structure type is built from $(Na_{3/4},Cd_{1/4})O_7$, $(Cd_{3/4},Na_{1/4})O_6$ and CdO_x (x 6, 7) polyhedra and PO_4 tetrahedra linked through common corners or edges. The resulting complex three dimensional framework consists of $[(Na_{3/4},Cd_{1/4})_2(Cd_{3/4},Na_{1/4})_2Cd_3O_{16}]_\infty$ layers stacked parallel to the (2 0—3) plane and interconnected both directly and via PO_4 tetrahedra by sharing common corners and edges. The vibrational spectroscopic results are in agreement with the factor group analysis and with the presence of two different PO_4^{3-} groups determined from the X ray diffraction study. Photoluminescence analysis evidences of two kinds of oxygen environments for the cadmium atoms, in line with the crystallographic description. The covalent character of this structure with its multiple sites occupied by cadmium cations should potentially make it a host material for optically active ions. As a consequence, attractive photoluminescence properties may be expected.

Appendix A. Supplementary data

Supplementary data to this article can be found online at https://doi.org/10.1016/j.molstruc.2019.126963.

References

[1] M. Kottaisamy, R. Jagannathant, P. Jeyagopal, R.P. Rao, R.L. Narayanan, Eu^{2+} luminescence in $M_5(PO_4)_3X$ apatites, where M is Ca^{2+}, Sr^{2+} and Ba^{2+} and X is F , CI , Br and OH , J. Phys. D Appl. Phys. 27 (1994) 2210 7215.
[2] X. Zhang, J. Zhang, J. Huang, X. Tang, M. Gong, Synthesis and luminescence of Eu^{2+}-doped alkaline-earth apatites for application in white LED, J. Lumin. 130 (2010) 554 559.
[3] J. Zhoua, Q. Liua, Z. Xia, Structural construction and photoluminescence tuning via energy transfer in apatite-type solid-state phosphors, J. Mater. Chem. C 6 (2018) 4371 4383.
[4] J. Lü, Y. Huang, L. Shi, H.J. Seo, The luminescence properties of Eu^{2+} doped $Na_2CaMg(PO_4)_2$ phosphor, Appl. Phys. A 99 (2010) 859 863.
[5] D. Geng, M. Shang, Y. Zhang, H. Lian, J. Lin, Temperature dependent luminescence and energy transfer properties of $Na_2SrMg(PO_4)_2$:Eu^{2+}, Mn^{2+} phosphors, Dalton Trans. 42 (2013) 15372 15380.
[6] A. Boukhris, B. Glorieux, M. Ben Amara, X-ray diffraction, ^{31}P NMR and europium photoluminescence properties of the $Na_2Ba_{1-x}Sr_xMg(PO_4)_2$ system related to the glaserite type structure, J. Mol. Struct. 1083 (2015) 319 329.
[7] M. Aboussatar, A. Mbarek, H. Naili, M. El-Ghozzi, G. Chadeyron, D. Avignant, D. Zambon, Phase equilibria in the NaF-CdO-$NaPO_3$ system at 873 K and crystal structure and physico-chemical characterizations of the new Na_2CdPO_4F fluorophosphate, J. Solid State Chem. 248 (2017) 75 86.
[8] G. Celotti, E. Landi, A misunderstood member of the nagelschmidtite family unveiled: structure of $Ca_5Na_2(PO_4)_4$ from X-ray powder diffraction data, J. Eur. Ceram. Soc. 23 (2003) 851 858.
[9] R. Widmer, F. Gfeller, T. Armbruster, Structural and crystal chemical investigation of intermediate phases in the system Ca_2SiO_4 $Ca_3(PO_4)_2$ $CaNaPO_4$, J. Am. Ceram. Soc. 98 12 (2015) 3956 3965.
[10] J. Yamakawa, T. Yamada, A. Kawahara, Un monophosphate de magnésium et sodium, Acta Crystallogr. C50 (1994) 986 988.
[11] A.G. Nord, P. Kierkegaard, The crystal structure of $Mg_3(PO_4)_2$, Acta Chem. Scand. 22 (1968) 1466 1474.
[12] L.N. Ji, H.W. Ma, J.B. Li, J.K. Liang, B.J. Sun, Y.H. Liu, J.Y. Zhang, G.H. Rao, A new structure type of phosphate: crystal structure of $Na_2Zn_5(PO_4)_4$, J. Solid State Chem. 180 (2007) 2256 2261.
[13] H.Y. Ng, W.T.A. Harrison, Monoclinic $NaZnPO_4$-ABW, a new modification of the zeolite ABW structure type containing elliptical eight-ring channels, Microporous Mesoporous Mater. 23 (1998) 197 202.
[14] Pechini M P. Method of Preparing Lead and Alkaline Earth Titanates and Niobates and Coating Method Using the Same to Form a Capacitor. US Patent. (1967) No.3.330.697.
[15] N. Walker, D. Stuart, An Empirical method for correcting diffractometer data absorption effets, Acta Crystallogr. A39 (1983) 158 166.
[16] A. Altomare, G. Cascarano, C. Giacovazzo, A. Guagliardi, Completion and refinement of crystal structures with SIR92, J. Appl. Crystallogr. 26 (1993) 343 350.
[17] G.M. Sheldrick, SHELXL-97, Program for Crystal Structure Refinement, University of Gottingen, Germany, 1997.
[18] R.D. Shannon, Revised effective ionic radii and systematic studies of interatomic distances in halides and chalcogenides, Acta Crystallogr. A32 (1976) 751 767.
[19] L.J. Farrugia, WinGX suite for small-molecule single-crystal crystallography, J. Appl. Crystallogr. 32 (1999) 837 838.
[20] R. Hoppe, S. Voigt, H. Glaum, J. Kissel, H.P. Müller, K. Bernet, A new route to charge distributions in ionic solids, J. Less Common. Met. 156 (1989) 105 122.
[21] M. Nespolo, G. Ferraris, G. Ivaldi, R. Hoppe, Charge distribution as a tool to investigate structural details. II. Extension to hydrogen bonds, distorted, and hetero-ligand polyhedra, Acta Crystallogr. B57 (2001) 652 664.
[22] A. Juhin, G. Morin, E. Elkaïm, D.J. Frost, M. Fialin, F. Juillot, G. Calas, Structure refinement of a synthetic knorringite, $Mg_3(Cr_{0.8}Mg_{0.1}Si_{0.1})_2(SiO_4)_3$, Am. Mineral. 95 (2010) 59 63.
[23] G. Donnay, R. Allmann, How to recognize O^2 , OH , and H_2O in crystal structures determined by x-rays, Am. Mineral. 55 (1970) 1003 1015.
[24] M. Ben Amara, R. Olazcuaga, G. Le Flem, M. Vlasse, The crystal structure of cadmium orthophosphate $Cd_4Na(PO_4)_3$, Acta Crystallogr. B35 (1979) 1567 1569.
[25] E. Holt, S. Drai, R. Olazcuaga, M. Vlasse, The crystal structure of cadmium orthovanadate $KCd_4(VO_4)_3$, Acta Crystallogr. B33 (1977) 95 98.
[26] Yu A. Ivanov, M.A. Simonov, N.V. Belov, Crystal structure of the Na,Cd orthophosphate $NaCdPO_4$, Kristallografiya 19 (1974) 163 164.
[27] W.H. Baur, The geometry of polyhedral distortions. Predictive relationships for the phosphate group, Acta Crystallogr. B30 (1974) 1195 1215.
[28] L. Elammari, B. Elouadi, Structure of $LiCdPO_4$, Acta Crystallogr. C44 (1988) 1357 1359 (E).
[29] M.P. Orlova, D.B. Kitaev, M.L. Spiridonova, N.V. Zubkova, Yu K. Kabalov, A.I. Orlova, Structure refinement of cadmium cerium(IV) phosphate $Cd_{0.5}Ce_2(PO_4)_3$, crystallogr, For. Rep. 50 (2005) 918 922.
[30] W.G. Fateley, F.R. Dollish, N.T. Mc Davitt, F.F. Bentley, Infrared and Raman Selection Rules for Molecular and Lattice Vibrations the Correlation Method, Wiley, New York, 1972.
[31] G. Venkataraman, V.C. Sahni, External vibrations in complex crystals, Rev. Mod. Phys. 42 4 (1970) 409 470.
[32] P. Tarte, A. Rulmont, C. Merckaert-ansay, Vibrational spectrum of nasicon-like,

rhombohedral orthophosphates $M^{I}M_2^{IV}(PO_4)_3$, Spectrochim. Acta 42A-9 (1986) 1009 1016.
[33] K. Nakamoto, Infrared and Raman Spectra of Inorganic and Coordination Compounds, fourth ed., Wiley & Sons, New York, 1986, p. 78.
[34] R.S. Halford, Motions of molecules in condensed systems: I. Selection rules, relative intensities, and orientation effects for Raman and infra-red spectra, J. Chem. Phys. 14 1 (1946) 8 15.
[35] V.S. Kurazhkovskaya, D.M. Bykov, E.Yu Borovikova, N.Yu Boldyrev, L. Mikhalitsyn, A.I. Orlova, Vibrational spectra and factor group analysis of lanthanide and zirconium phosphates $M^{III}_{0.33}Zr_2(PO_4)_3$, where M^{III} Y, La Lu, Vib. Spectrosc. 52 (2010) 137 143.
[36] A. Jillvenkatesa, R.A. Condrate Sr., The Infrared and Raman spectra of β- and α-tricalcium phosphate ($Ca_3(PO_4)_2$), Spectrosc. Lett. 31 8 (1998) 1619 1634.
[37] Y. Yonesaki, C. Matsuda, Crystal structure of $Na_2MMgP_2O_8$ (M: Ba, Sr, Ca) orthophosphates and their luminescence properties by Eu^{2+}; analogous structural behaviors of glaserite-type phosphates and silicates, J. Solid State Chem. 184 (2011) 3247 3252.
[38] M. Barj, G. Lucazeau, C. Delmas, Raman and infrared spectra of some chromium nasicon-type materials: short-range disorder characterization, J. Solid State Chem. 100 (1992) 141 150.
[39] K. Narita, Luminescence of Ag-exchanged zeolite 13X, J. Lumin. 4 (1971) 73 80.
[40] E. Radzhabov, M. Kirm, Triplet luminescence of cadmium centres in alkaline-earth fluoride crystals, J. Phys. Condens. Matter 17 (2005) 5821 5830.